Controlling the Femtochemistry of $Fe(CO)_5$

M. Bergt, T. Brixner, B. Kiefer, M. Strehle, and G. Gerber*

Physikalisches Institut, Universität Würzburg, Am Hubland, D-97074 Würzburg, Germany

Received: July 22, 1999; In Final Form: September 23, 1999

We report on active control of the femtosecond photodissociation and ionization reactions of iron pentacarbonyl, $Fe(CO)_5$, in the gas phase. The spectral phase of femtosecond laser pulses is modified in a pulse shaper, employing a learning evolutionary algorithm. Direct feedback from the experiment is used to iteratively improve the laser pulse shape according to a given optimization problem. This many-parameter optimization is compared with one-parameter control schemes and found to be more versatile, because it can sample a much more general search space. Information about the underlying reaction mechanism can be extracted from the results of the automated optimization. It is further shown that second-harmonic generation (SHG) can be used at the output of a 800 nm pulse shaper to implement 400 nm excitation experiments. The optimization procedure not simply increases the SHG efficiency but optimizes the objective given for the combined system of SHG and $Fe(CO)_5$ photochemistry. The importance of the choice of fitness function is examined experimentally. By choosing appropriate weighting factors, it is possible to tune the optimization results from an optimization of the ratio of photoproduct yields toward optimization of the absolute photoproduct yields. Evolutionary laser pulse shaping is considered a very useful tool for unraveling the processes of photoinduced chemical reactions.

1. Introduction

Controlling the outcome of chemical reactions by specifically tailored femtosecond laser pulses is a fascinating perspective which has recently become experimentally feasible. The beginnings of the so-called concept of "coherent control"[1−3] can be summarized as follows. It was shown theoretically by Brumer and Shapiro[4−6] that by exciting a quantum-mechanical system with phase-related continuous-wave lasers it is possible to obtain constructive or destructive quantum interference for specific reaction pathways, depending on the relative phase of the lasers. Experimental realizations were demonstrated on atomic and small molecular systems.[7,8] Tannor, Kosloff, and Rice[9,10] suggested a time-domain approach, where the variation of the delay between two ultrashort laser pulses is exploited in a "pump−dump scheme". This has also been realized experimentally by several groups.[11−14] A new approach was made by Rabitz and co-workers[15,16] who proposed to use optimal control theory to specifically design ultrashort laser pulses for control purposes. Molecular vibrational wavepackets should thus be prepared and "steered" into the desired exit channel.[15−17] Experiments with linearly chirped laser pulses have shown promising results.[18−22] However, calculating the electric fields for a given control problem is quite a complicated task, especially since potential energy surfaces of complex molecules are usually not known accurately enough.

Judson and Rabitz[23] therefore introduced the idea to directly include the experimental output in the optimization procedure of the electric field. Femtosecond laser pulses, modified by a pulse shaping device, are used to excite the molecular system. The individual yields of the resulting photoproducts are then used as feedback in a learning algorithm which iteratively improves the shape of the applied laser pulses until an optimum is reached. Since no knowledge about the molecular Hamiltonian or the experimental environment is required but rather the computer algorithm solves the optimization problem, this concept may be called "automated coherent control". The usefulness of evolutionary algorithms as optimization algorithms has been demonstrated in the case of automated femtosecond pulse compression.[24−27] Wilson and co-workers[28] have been the first to use automated pulse shaping to optimize the electronic population transfer in a dye molecule. We have recently realized automated coherent control of chemical reactions,[29,30] optimizing final product yields in the photodissociation reactions of two different organometallic molecules. Tailored femtosecond laser pulses were also used to control two-photon transitions in cesium gas.[31]

Besides controlling chemical reaction dynamics by laser radiation, it is a major issue to understand the fundamental processes the molecular system undergoes during and after the interaction with the shaped laser pulses. One possible method of investigation might be to carry out a whole series of optimization experiments with varying parameters such as wavelength, pulse energy, fitness function, etc. and to try to find out if these different experiments exhibit common features in the experimental output such as the product branching ratios, the development of the fitness value during the optimization, the resulting laser pulse shape, and so on. We illustrate some of these issues on the example of iron pentacarbonyl, $Fe(CO)_5$.

The organization of this paper is as follows. Section 2 briefly sketches the experimental setup and describes the pulse shaper. In section 3, we review the possibilities of one-parameter laser control in terms of wavelength, pump−probe delay, pulse energy, and pulse duration. Particularly, we show that the $Fe(CO)_5$ dissociation reaction cannot be described as simply "intensity-dependent", because different types of intensity variation lead to completely opposite behavior. In section 4, our implementation of the evolutionary algorithm is described,

* Corresponding author. Fax: +49-931-888-4906. E-mail: gerber@physik.uni-wuerzburg.de.

10.1021/jp992541k CCC: $18.00
Published on Web 11/03/1999

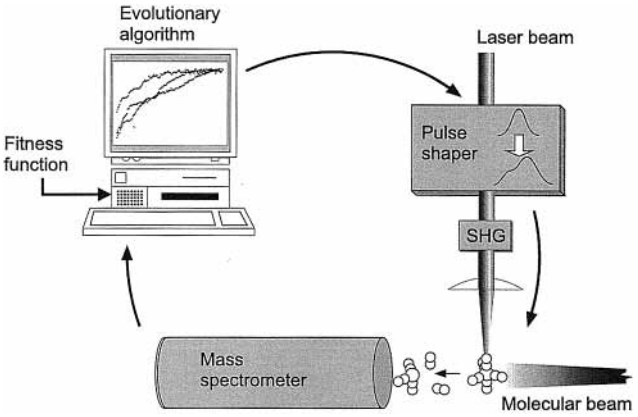

Figure 1. Experimental setup. Femtosecond laser pulses are modified in a pulse shaper and optionally frequency-doubled. After interaction with a molecular beam of $Fe(CO)_5$ in a high-vacuum chamber, the ionic photoproduct yields are detected with a reflectron time-of-flight (TOF) mass spectrometer and used as feedback in an evolutionary computer algorithm. The laser pulse shape and therefore the product yield is optimized iteratively, according to a specific fitness function.

and the question of the choice of a suitable fitness function is addressed. Section 5 compares our previous results[30] from the automated 800 nm optimization of the $Fe(CO)_5^+/Fe^+$ ratio with new results obtained with a slightly different fitness function. We describe how for this specific molecule, the dynamics of the fundamental reaction mechanism can be inferred from the optimization results (the so-called "problem of inversion"). Further on, we show that it is possible to use second-harmonic generation (SHG) between the pulse shaper and the molecular beam apparatus to optimize dissociation reactions with 400 nm phase-shaped laser pulses. The algorithm not simply optimizes SHG efficiency but instead finds solutions optimal to the combined system of SHG and photodissociation processes. It is possible to adjust the balance between optimization of the desired branching ratio and maximization of the total (absolute) fragment yield by a suitable choice of weighting parameters in the fitness function.

2. Experiment

The experimental setup is sketched in Figure 1. Our laser system consists of a home-built Ti:sapphire oscillator and a chirped-pulse amplification (CPA) system providing 80 fs, 1 mJ pulses at a center wavelength of 800 nm and a repetition rate of 1 kHz. These pulses are modified in a femtosecond phase shaper based on a design of Weiner et al.[32,33] Pulse-shaping techniques for simultaneous amplitude and phase shaping[34] as well as pulse shapers with acousto-optic modulators (AOM)[35] have also been developed, but are not used here. As described previously,[27] we use a zero-dispersion compressor set up with 1800 lines/mm gratings and 80 mm plano-cylindrical lenses to disperse and recollimate the femtosecond pulse spectrum. A liquid-crystal display (LCD), model SLM-128 by Cambridge Research and Instrumentation (CRI), is used as phase modulator in the Fourier plane. By applying different voltages to the 128 independent pixels of the LCD array, their refractive indices can be changed. Different optical path lengths are thus introduced to the spatially separated spectral components, allowing for almost arbitrary spectral phase modulation. In the time domain, this leads to a redistribution of the laser pulse energy (and therefore to different pulse lengths and pulse shapes) as well as to temporal chirp. Since we do not use the LCD as an amplitude modulator but only as a phase modulator, the total pulse energy is independent of the introduced chirp. With our setup we achieve an energy throughput of 68%. The output pulses are used either directly or after subsequent second-harmonic generation (SHG) where the fundamental has been removed afterwards. Of course it would be preferable to directly phase-shape the 400 nm laser pulses. This is difficult with the present LCD, however, because at a wavelength of 400 nm the absorption of light by the liquid-crystal molecules is no longer negligible.

The $Fe(CO)_5$ molecules are investigated in the gas phase by employing a molecular beam apparatus with a reflectron time-of-flight (TOF) mass spectrometer.[36] All mass spectra are obtained by focusing the modulated laser pulses into the interaction region with a 300 mm quartz lens. In the automated coherent control experiments, a computer algorithm uses the mass spectra as feedback in a learning algorithm as described in section 4.

Following 800 or 400 nm femtosecond pulse excitation in the gas phase, $Fe(CO)_5$ shows different ionization and fragmentation processes.[37] Direct ionization leads to $Fe(CO)_5^+$ whereas combined ionization and fragmentation leads to $Fe(CO)_n^+$, $n = 0, 1, 2, 3, 4$. In this paper, we concentrate on the competing processes of direct ionization, yielding $Fe(CO)_5^+$, and complete dissociation, leaving only the bare Fe^+. For the sake of simplicity, we omit the "+" signs throughout the text and use the term "$Fe(CO)_5$/Fe ratio" to describe the quotient of the ionic mass signals $Fe(CO)_5^+$ and Fe^+.

3. One-Parameter Control Mechanisms

Historically, one of the first control parameters introduced was the wavelength. Indeed, in the early days of mode-selective chemistry it was thought that by tuning monochromatic laser light according to the "mode frequency" of a chemical bond, selective dissociation could be achieved.[38−40] Although in most cases selectivity is lost because of intramolecular vibrational redistribution (IVR),[1,41] the excitation wavelength plays an important role also in coherent control experiments with femtosecond laser pulses. Depending on the center wavelength of the broadband laser pulse spectrum, vibrational wavepackets can be prepared in different transition states, some of which might be better suited to achieve a given optimization task. In the case of $Fe(CO)_5$, we observed different photoproduct distributions after single-pulse 800 and 400 nm excitation.[37]

The pump−probe technique, used to determine the dynamics of photodissociation processes, can sometimes be used as an easy way to influence the product distribution as suggested by Tannor, Kosloff, and Rice.[9,10] We have investigated the effect of pump−probe delay on the distribution of the photoproducts of $Fe(CO)_5$.[37,42] Summarizing, for 400 nm multiphoton excitation and a 800 nm probe step, the $Fe(CO)_5$ ion yield is maximal for overlapping pump and probe laser pulses. With increasing pump−probe delay, the maximum ion yields are reached sequentially, first for $Fe(CO)_n$, $n = 2, 3, 4$, then for Fe(CO), and finally for Fe. Different fragment ratios can thus be realized by choosing suitable pump-probe delays.

At least in some cases, an increased pulse duration can be thought of as being made of a sequence of bandwidth-limited laser pulses (such as used in pump−probe experiments). From the preceding discussion it is therefore clear that the pulse duration in a single-pulse experiment can have a strong effect on the photoproduct distribution and can in fact be used as a control parameter. If the laser pulse duration is increased (as can be done with a phase shaper), the temporal intensity is decreased. Lowering the intensity is also possible by reducing the pulse energy at constant pulse duration. These two pos-

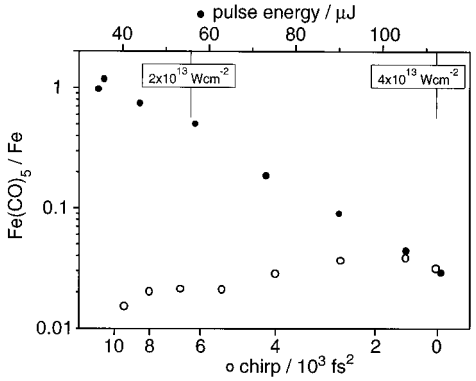

Figure 2. Pulse energy and pulse length dependence of the $Fe(CO)_5$/Fe ratio using 800 nm laser pulses.

sibilities of lowering the laser intensity must not be confused, however, because they lead to totally different responses of the sample substance, as we will show in the following.

We have first generated 800 nm bandwidth-limited laser pulses by automated femtosecond pulse compression, as described elsewhere.[27] Starting from there we performed two experiments of one-parameter control of the $Fe(CO)_5$ dissociation branching ratios. First, by applying different attenuations to the laser beam, we varied the pulse energy in an interval from 113 to 34 μJ. With the measured temporal pulse shape (employing the SHG-FROG technique) and a focus diameter of about 100 μm in the interaction region, the different pulse energies can be transformed into intensities. Second, by applying with our pulse shaper additional linear chirp in the range of $0-10^4$ fs^2 at a constant pulse energy of 113 μJ, the pulse duration and therefore also the intensity can be varied. In principle, this experiment could also be done by a conventional prism compressor. Therefore, we present these results in this section of one-parameter control schemes. The ratios of $Fe(CO)_5$/Fe achieved in the two experiments are shown in Figure 2. Both schemes exhibit a completely different behavior. Whereas reducing the pulse energy (and therefore reducing the intensity) leads to an increased $Fe(CO)_5$/Fe ratio, increasing the pulse duration by introducing linear chirp (and therefore as well reducing the intensity) leads to a decreased $Fe(CO)_5$/Fe ratio. Hence, it is not quite correct to speak of the $Fe(CO)_5$/Fe ratio as intensity-dependent, since different types of intensity variation lead to a different behavior.

We conclude that by using phase-shaped femtosecond laser pulses on $Fe(CO)_5$, processes can be induced and studied which are not accessible by a variation of the pulse energy alone. Automated optimization of the $Fe(CO)_5$/Fe ratio using 800 nm laser pulses will be discussed in section 5.1.

Similar experiments can be done with 400 nm laser pulses. The effect of laser pulse energy on the absolute ion yield of $Fe(CO)_5$ and Fe is illustrated in Figure 3a. With increasing pulse energy, both signals increase, but with a different slope. The corresponding $Fe(CO)_5$/Fe ratio is shown in Figure 3b. By adjusting the laser pulse energy between 38 and 6 μJ, it is possible to change the $Fe(CO)_5$/Fe ratio from 0.25 to 1.35. This result, together with the absolute ion yield, will be compared with the result of the corresponding automated 400 nm optimization in section 5.2.

4. Evolutionary Pulse Shaping

Each of the "simple" control mechanisms discussed so far makes use of only one control parameter. Usually this is not sufficient for more complex molecules. By controlling the phase

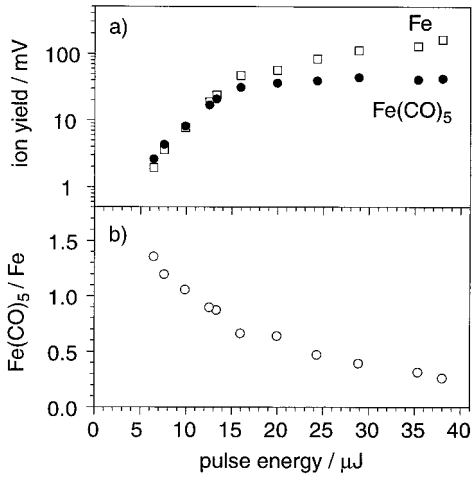

Figure 3. Pulse energy dependence of the absolute $Fe(CO)_5$ and Fe signals (a) and the corresponding $Fe(CO)_5$/Fe ratio (b) using 400 nm laser pulses.

of the femtosecond laser pulses over the whole spectrum, the number of independent parameters can be greatly increased. As will be shown in the case of $Fe(CO)_5$, automated control with the aid of a programmable pulse shaper may improve the final result of the optimization.

An evolutionary algorithm is an optimization method which mimics processes of the biological evolution.[43,44] We have described our implementation in detail elsewhere.[25] Briefly, the "genetic configuration" of an "individual" consists of the 128 voltage values applied to the LCD array. The modulated laser pulse is used to excite the molecule under examination, and the resulting distribution of the photoproducts is then used to calculate a certain fitness function (see below). The higher the fitness is, the better the laser pulse is suited to achieve the objective to a given optimization problem. After testing all individuals of one generation (randomly initialized), the best ones are selected for reproduction according to the evolutionary principle of the "survival of the fittest". Crossover and mutation procedures lead to offspring which is often better adapted to the environment than its precursors. Again, all individuals are tested, and the best of them are selected. After many iterations of the evolutionary process, the average fitness has increased and the goal of the optimization problem is achieved.

In our previous work on automated pulse compression, the fitness was simply set equal to the amount of SHG light produced by the modulated laser pulses.[25,27] The shorter the laser pulses were, the more SHG could be detected. In this way, the target of bandwidth-limited laser pulses could be reached. In the case of coherent control, we maximized (and minimized) the ratio of two selected photoproduct yields, thereby favoring the reaction product of the numerator over the reaction product of the denominator (and vice versa).[29,30]

In some cases, these "standard" fitness functions may not be sufficient. For example, the quotient can get very large (thereby indicating a high fitness) if the denominator gets very small. In our context, the optimization target could be reached by essentially producing nothing of the product in the denominator (which is of course what is wanted), but also producing almost nothing of the product in the numerator (which is usually not wanted). We have avoided this problem by introducing a more versatile fitness function.

We now use a fitness function of the form $f(x,y) = ax/y + bx + cy$ where x and y indicate the measured fragment yields of the desired and undesired reaction products, respectively, and

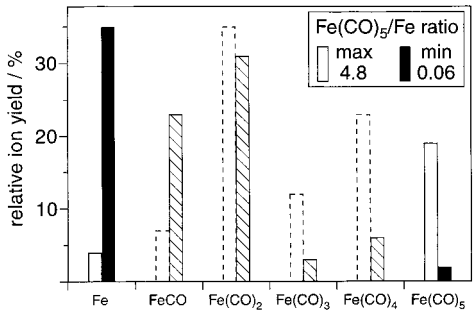

Figure 4. Relative photoproduct distribution after automated maximization and minimization of the $Fe(CO)_5$/Fe ratio using 800 nm laser pulses and $y_0 = 0$ in the fitness function.

a, *b*, and *c* are suitable parameters. Additionally, we can replace *y* in the term *x*/*y* by some threshold value y_0 whenever $y < y_0$. If $a > 0$ and $b = c > 0$, for example, not only the ratio of the fragments but also their total yield is maximized. By adjusting *a* on the one hand and *b* and *c* on the other hand, the relative importance of total signal maximization with respect to maximization of the photoproduct ratio can be chosen. The threshold value y_0 prevents *x*/*y* from getting very high if *x* and *y* both are below the noise level, with *x* being only accidentally higher. If no positive threshold is used, the evolutionary algorithm may find an optimum with very small total yields. The ratio actually goes to infinity if *y* tends to zero. The application of this generic fitness function with different parameter values is shown in the next section.

5. Automated Coherent Control

5.1. Optimization with 800 nm Laser Pulses. The results of the maximization and minimization of the $Fe(CO)_5$/Fe ratio using 800 nm laser pulses and fitness parameters $a > 0$, $b = c = 0$, and $y_0 = 0$ are shown in Figure 4 as published previously.[29,30] Significantly different product distributions are achieved in the two cases, with the $Fe(CO)_5$/Fe ratio dropping from 4.8 in the maximization experiment toward 0.06 in the minimization experiment. The corresponding laser pulse shape is bandwidth-limited in the case of maximization,[29] found after about 30 generations of the evolutionary process. In the minimization experiment, arbitrarily long laser pulses of picosecond duration are sufficient,[29] which means that the algorithm essentially produces the best result already in the first few generations. Since we have not used a threshold value (i.e., $y_0 = 0$), high ratios (and therefore high fitness values) are possible with small total ion yield. In the mass spectrum leading to Figure 4 ($Fe(CO)_5$/Fe minimization), for instance, the $Fe(CO)_5$ peak is barely above the noise level (note that the relative ion yields are plotted). When we repeated the experiment, again with $a > 0$ and $b = c = 0$ but with a threshold value $y_0 > 0$ that was chosen such as to allow only signals above the noise floor to enter the calculation of the fitness function, the final product distribution (not shown here) exhibited a maximized $Fe(CO)_5$/Fe ratio of 2.2 and a minimized ratio of 0.2. As expected, the ratios were not as extreme as without using the threshold procedure, but the total yield was considerably higher. This is due to the fact that in the $Fe(CO)_5$/Fe minimization procedure, the algorithm could not get "stuck" with arbitrarily long laser pulses already in the first few generations. Note that it is difficult to compare the ratios of the former and the new experiments directly, because we now use an improved pulse shaper setup with cylindrical lenses,[27] allowing higher output energies. Other experimental parameters such as the molecular beam density

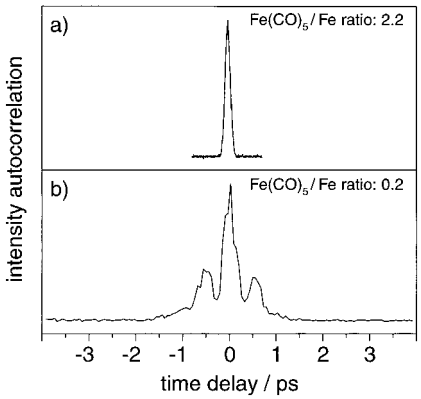

Figure 5. Autocorrelation functions from a 800 nm maximization (a) and minimization (b) of the $Fe(CO)_5$/Fe ratio using $y_0 > 0$ in the fitness function.

and so on may also be different. Evolutionary algorithms of course search for optimum results within the given experimental parameters.

The results may also be discussed in view of the corresponding laser pulse shapes. The $Fe(CO)_5$ experiments may present an example where it is possible to extract information about the reaction mechanism from the results of the optimization. Intensity autocorrelations of the maximization as well as the minimization experiment using $y_0 > 0$ are shown in Figure 5. In the case of $Fe(CO)_5$/Fe maximization, a bandwidth-limited laser pulse is produced (Figure 5a) as in the former experiment with $y_0 = 0$. This is no surprise because according to Figure 2 the shortest possible laser pulse leads to the highest $Fe(CO)_5$/Fe ratio. On the other hand, for a minimization of the $Fe(CO)_5$/Fe ratio, longer laser pulses are needed according to Figure 2. In the case of $y_0 = 0$ this led to an arbitrarily long laser pulse where the $Fe(CO)_5$/Fe ratio is lowest. But with $y_0 > 0$ this is no longer possible, and another optimum has to be found. The autocorrelation function shown in Figure 5b exhibits a three-peak structure with temporal spacings of about 500 fs. This is indicative of a double-pulse laser intensity profile with one pulse delayed by 500 fs from the other. Note that the double-pulse is produced by the pulse shaper from a single input laser pulse. The optimization results can be understood in terms of the pump−probe experiments published earlier.[37,42] A detailed theoretical interpretation of these experimental pump−probe investigations will be given in ref 45. With increasing pump−probe delay the maximum of the photoproduct distribution shifts toward smaller fragments. Therefore if the $Fe(CO)_5$/Fe ratio is to be made small, longer pump−probe delays are needed. This is exactly what can be seen in the double-pulse structure. On the other hand, if the $Fe(CO)_5$/Fe ratio is to be made large, short pump−probe delays (or essentially overlapping pulses) are needed. Again, this is in agreement with the single bandwidth-limited laser pulse produced in the maximization experiment.

It is possible to give a physical explanation for these optimization results. In a first step, multiphoton absorption in the parent molecule initiates some wavepacket dynamics on a neutral dissociative potential energy surface. Theoretical investigations[45] show that the molecule may be excited simultaneously to more than one potential energy surface. It takes then some time for the wavepacket to move on the surface(s) and to reconfigure the molecule such that the iron−carbonyl bonds are broken, before in a second step the resulting fragments are detected by multiphoton ionization. For complete fragmentation, the temporal separation between these two steps can be

approximately determined from Figure 5. This separation is shorter than 500 fs (the time-delay between the two pulses forming the structure of Figure 5b), but longer than 100 fs (the pulse duration which is visible in Figure 5a). If the time scale for the bond breakings were longer than 500 fs, it should show up in an increased separation of the double-pulse structure in the minimization experiment; if the time scale were shorter than 100 fs, the additional structure at 500 fs delay should have no effect on the $Fe(CO)_5$/Fe ratio, except that the energy in the first part of the double pulse were lower. According to Figure 2, however, reducing the energy would again lead to a maximization instead of a minimization of the $Fe(CO)_5$/Fe ratio. Therefore, the assumption about the time scales and the underlying dynamics should be correct. Since our pulse shaper does not modulate amplitudes, pulse shapes different from the (optimal) pump−probe of Figure 5b would imply a redistribution of temporal intensity. The intensity in the pump and/or in the probe step would decrease and the probability of transfer to the excited and the final states, respectively, would drop, leading to a less than optimal branching ratio or total ion yield. What can be learned about the $Fe(CO)_5$ molecule then is that within the wide class of possible laser pulse shapes accessible by the pulse shaper, a pump−probe scheme represents a very efficient mechanism for population transfer from the initial state $Fe(CO)_5$ to the final state Fe.

In the case of $Fe(CO)_5$/Fe maximization, the wavepacket has not evolved significantly within the duration of the single laser pulse. Further evolution is stopped as the momentary configuration (at under 100 fs still the undissociated parent molecule) is projected into the ionic continuum. Therefore, mainly $Fe(CO)_5$ is detected. The remaining fragments are due to dissociative ionization. Indeed, our previous pump−probe experiments[37,42] yielded fragmentation times of 100 fs for the first four iron−carbonyl bonds, and 230 fs for the last bond, altogether within the limits deduced from the automated control experiments. In light of the completely opposite behavior of the $Fe(CO)_5$/Fe ratio with the two types of varying laser "intensity" shown in Figure 2, we think that an explanation of the optimization results by "static" intensity-dependent multiphoton absorption probabilities can be excluded, and the more complex "dynamical" picture described above is applicable. The deductions drawn in this "simple" example of $Fe(CO)_5$ dissociation may therefore be viewed as a step toward the qualitative solution of the so-called "problem of inversion" of automated optimization, i.e., finding the fundamental mechanisms from the optimization results. Further investigations are necessary to establish evolutionary pulse shaping as a general tool for answering these types of questions.

5.2. Optimization with 400 nm Laser Pulses. In order to illustrate that it is possible to do automated coherent control experiments with wavelengths other than 800 nm, we frequency-doubled the output of the pulse shaper in a nonlinear LBO crystal before focusing it into the interaction region. Two aspects have to be taken into account. On the one hand, a specific chirp might improve the interaction, but on the other hand the SHG efficiency is strongly dependent on the chirp. Here we demonstrate that if the 400 nm pulses are used in coherent control experiments, maximization of a given objective (such as maximization of a photoproduct yield ratio) does not simply lead to bandwidth-limited pulses, but rather to a specifically phase-shaped 400 nm laser pulse optimal to the given problem. In other words, the combined system of SHG and molecular $Fe(CO)_5$ photodissociation is optimized by this procedure, not just the SHG efficiency itself.

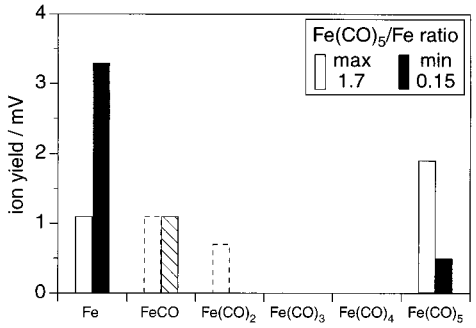

Figure 6. Absolute photoproduct distribution after automated maximization and minimization of the $Fe(CO)_5$/Fe ratio using 400 nm laser pulses and low values of b and c in the fitness function.

In the following series of experiments we chose a suitable threshold value $y_0 > 0$ for the reasons discussed above. We then performed optimization experiments with $x = Fe(CO)_5$ and $y = Fe$ (which are referred to as "maximization" experiments, because the ratio $Fe(CO)_5$/Fe is maximized) as well as with $x = Fe$ and $y = Fe(CO)_5$ (which are referred to as "minimization" experiments, because the ratio $Fe(CO)_5$/Fe is minimized). The relative importance of absolute signal maximization with respect to photoproduct ratio maximization was varied from "low" to "high", employing three different parameter sets a, b, and c.

First, we chose $a = 1$ and $b = c$ such that $ax/y > bx + cy$ for unmodulated laser pulses, meaning that the improvement of the ratio was given more weight than the maximization of the absolute signal. The resulting product distribution is given in Figure 6 showing the absolute signals from the mass spectra. In the maximization experiment, a $Fe(CO)_5$/Fe ratio of 1.7 is achieved, whereas in the minimization experiment the ratio is 0.15.

The first observation is that going from the automated $Fe(CO)_5$/Fe maximization results to the minimization results, the absolute $Fe(CO)_5$ yield decreases whereas the absolute Fe yield increases. This behavior is different from Figure 4 where only the relative yield showed qualitatively similar behavior but the total yield was lower in the minimization experiment (by a factor of about 10). We attribute this to the use of the threshold value $y_0 > 0$ which prevents the evolutionary algorithm from simply producing a very long laser pulse (with corresponding low intensity and low total yield).

The second observation is that in the one-parameter control experiment of pulse energy variation (Figure 3b), we could change the $Fe(CO)_5$/Fe ratio between 0.25 and 1.35 in the examined energy range. The results obtained with the pulse shaper are slightly better, but it cannot be excluded that this is an effect of uncompensated chirp of the 400 nm pulses in the energy attenuation experiment, due to the LBO crystal. However, even if we extrapolate Figure 3b and imagine the ratios from the automated optimization to be reached, the absolute yields (Figure 3a) are drastically different for the $Fe(CO)_5$/Fe maximization (<3 mV) and minimization (>40 mV). Using energy attenuation alone, it is not possible to obtain the pulse shaper result of maximized and minimized ratios and to simultaneously achieve almost equal total yields. The conclusion is that by using a femtosecond phase shaper with an evolutionary algorithm, ionization/fragmentation processes of $Fe(CO)_5$ are accessible that cannot be initiated by bandwidth-limited laser pulses of varying energy.

In the second set of the optimization series, we chose moderately higher values of $b = c$ such that $ax/y < bx + cy$ for unmodulated laser pulses. Again we wanted to maximize and minimize the $Fe(CO)_5$/Fe ratio, but with an increased weight

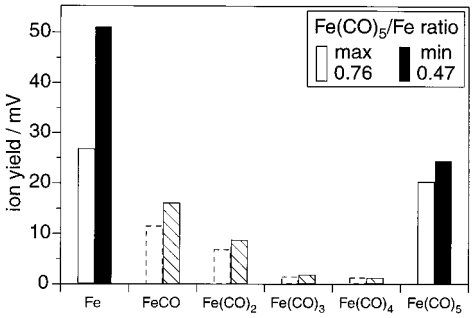

Figure 7. Absolute photoproduct distribution after automated maximization and minimization of the $Fe(CO)_5$/Fe ratio using 400 nm laser pulses and medium values of *b* and *c* in the fitness function.

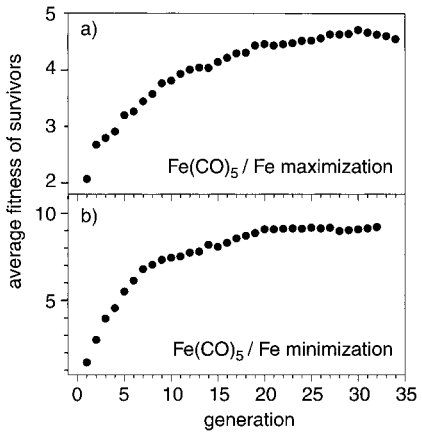

Figure 8. Evolution of the fitness function leading to the photoproduct distribution of Figure 7 for the case of $Fe(CO)_5$/Fe maximization (a) and minimization (b).

on the absolute ion signal. The results are shown in Figure 7. As before, maximization as well as minimization is possible. But additionally, the absolute signal is greatly enhanced, as was requested by the fitness function. However, the increase of the absolute signal is at the cost of the maximum and minimum ratios, which are not as good as in the case of Figure 6. The maximized ratio (0.76) is higher than the ratio obtained with a nonmodulated laser pulse, and the minimized ratio (0.47) is lower. This implies again a true optimization. Since the experimental conditions such as the molecular beam density, the laser pulse energy, and so on were not stable enough to achieve the same absolute signals over the whole period of this experimental series, the results of this second and the following third step should not directly be compared to the energy variance scheme from Figure 3.

The typical evolution of the fitness function is shown for the maximization (Figure 8a) as well as the minimization experiment (Figure 8b) leading to the photoproduct distribution of Figure 7. Depending on the fitness parameters, these curves may exhibit more fluctuations, especially if y_0 is chosen too low, and thus small signals lead to a high uncertainty in the x/y ratio. It can also be seen from Figure 8 that arbitrarily phase-shaped laser pulses (as produced in the first generation of the evolutionary process) are not sufficient for either the maximization or the minimization experiment. If arbitrarily phase-shaped laser pulses were sufficient, at least one of the curves would not show a clear rise with increasing number of generations.

In the third step we further increased the magnitude of *b* and *c* with respect to the previous step. This time, almost all weight of the fitness function is put onto the absolute signal whereas the photoproduct yield ratio is not very important. The results are shown in Figure 9. Since high absolute signals are wanted,

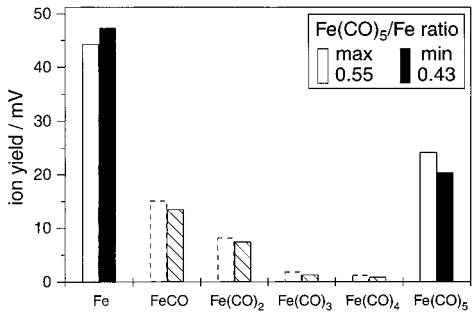

Figure 9. Absolute photoproduct distribution after automated maximization and minimization of the $Fe(CO)_5$/Fe ratio using 400 nm laser pulses and high values of *b* and *c* in the fitness function.

high laser intensities (and therefore short laser pulses) are required in both cases. This means that essentially both the maximization and the minimization procedures try to compress the femtosecond laser pulses. Even though this is the case (the absolute signals both reach almost the same level as for no additional phase modulation), the $Fe(CO)_5$/Fe ratio can still be varied, but in a further limited range from 0.43 in the case of minimization to 0.55 in the case of maximization.

As an overall result of this series, we recognize that by choosing the correct weighting factors in the fitness function, it is possible to tune automated coherent control experiments from an optimization of mainly the photoproduct yield ratios toward optimization of the absolute mass signal.

6. Conclusion

In this paper, we used a femtosecond laser pulse shaper in combination with an evolutionary algorithm and feedback from the experimental output in order to investigate and actively control the $Fe(CO)_5$ ionization and fragmentation processes. In particular, we have shown that the $Fe(CO)_5$/Fe ratio cannot be described as simply "intensity"-dependent, because intensity alteration by pulse energy variation leads to a behavior opposite to intensity alteration by pulse duration variation. Phase modulation of the 800 nm laser pulses can therefore be used to induce processes other than by simple pulse energy reduction. This fact is used in the automated control experiments where optimum $Fe(CO)_5$/Fe ratios are found in either direction. The resulting laser pulse shapes give valuable clues about the dynamics of the underlying physical processes. Iron pentacarbonyl can be regarded as a simple example where the "problem of inversion" can be tackled. Further investigations in this general direction are necessary to fully clarify the different fragmentation processes of $Fe(CO)_5$.

We further explored the possibility of using second-harmonic generation after the pulse shaper to produce 400 nm phase-shaped laser pulses for automated coherent control experiments. It was shown that this is indeed possible and that optimization of a given objective of quantum control does not simply lead to a maximization of the SHG efficiency but instead to an optimization of the combined system of SHG and molecular fragmentation/ionization of $Fe(CO)_5$. Varying the weighting parameters of the fitness function, it is possible to choose between mainly optimization of the $Fe(CO)_5$/Fe ratio (not demanding high total yield) and mainly maximization of the absolute yield (where the ratio is not considered as important).

Future experiments might, for example, address the question of how product branching ratios other than $Fe(CO)_5$/Fe can be optimized by phase-shaped laser pulses and if their changes can be made to surpass the changes they undergo in the $Fe(CO)_5$/Fe optimization experiments discussed here.

We consider evolutionary pulse shaping a very useful tool which will play an increasingly important role in unraveling the secrets of photoinduced chemical reactions.

Acknowledgment. We acknowledge stimulating discussions with the members of the SFB 347 "Selektive Reaktionen Metall-aktivierter Moleküle" at the University of Würzburg as well as generous financial support from the Fonds der chemischen Industrie.

References and Notes

(1) Warren, W. S.; Rabitz, H.; Dahleh, M. *Science* **1993**, *259*, 1158.
(2) Gordon, R. J.; Rice, S. A. *Annu. Rev. Phys. Chem.* **1997**, *48*, 601.
(3) Zare, R. N. *Science* **1998**, *279*, 1875.
(4) Brumer, P.; Shapiro, M. *Chem. Phys. Lett.* **1986** *126*, 541.
(5) Shapiro, M.; Hepburn, J. W.; Brumer, P. *Chem. Phys. Lett.* **1988**, *149*, 451.
(6) Brumer, P.; Shapiro, M. *Chem. Phys.* **1989**, *139*, 221.
(7) Chen, C.; Yin, Y.-Y.; Elliott, D. S. *Phys. Rev. Lett.* **1990**, *64*, 507.
(8) Park, S. M.; Lu, S. P.; Gordon, R. J. *J. Chem. Phys.* **1991**, *94*, 8622.
(9) Tannor, D. J.; Rice, S. A. *J. Chem. Phys.* **1985**, *83*, 5013.
(10) Tannor, D. J.; Kosloff, R.; Rice, S. A. *J. Chem. Phys.* **1986**, *85*, 5805.
(11) Baumert, T.; Grosser, M.; Thalweiser, R.; Gerber, G. *Phys. Rev. Lett.* **1991**, *67*, 3753.
(12) Potter, E. D.; Herek, J. L.; Pedersen, S.; Liu, Q.; Zewail, A. H. *Nature* **1992**, *355*, 66.
(13) Baumert, T.; Gerber, G. *Isr. J. Chem.* **1994**, *34*, 103.
(14) Herek, J. L.; Materny, A.; Zewail, A. H. *Chem. Phys. Lett.* **1994**, *228*, 15.
(15) Shi, S.; Woody, A.; Rabitz, H. *J. Chem. Phys.* **1988**, *88*, 6870.
(16) Peirce, A. P.; Dahleh, M. A.; Rabitz, H. *Phys. Rev. A* **1988**, *37*, 4950.
(17) Kosloff, R.; Rice, S. A.; Gaspard, P.; Tersigni, S.; Tannor, D. J. *Chem. Phys.* **1989**, *139*, 201.
(18) Kohler, B.; Yakovlev, V. V.; Che, J.; Krause, J. L.; Messina, M.; Wilson, K. R.; Schwentner, N.; Whitnell, R. M.; Yan, Y. *Phys. Rev. Lett.* **1995**, *74*, 3360.
(19) Bardeen, C. J.; Wang, Q.; Shank, C. V. *Phys. Rev. Lett.* **1995**, *75*, 3410.
(20) Assion, A.; Baumert, T.; Helbing, J.; Seyfried, V.; Gerber, G. *Chem. Phys. Lett.* **1996**, *259*, 488.
(21) Blanchet, V.; Bouchène, M. A.; Cabrol, O.; Girard, B. *Chem. Phys. Lett.* **1995**, *233*, 491.
(22) Pastirik, I.; Brown, E. J.; Zhang, Q.; Dantus, M. *J. Chem. Phys.* **1998**, *108*, 4375.
(23) Judson, R. S.; Rabitz, H. *Phys. Rev. Lett.* **1992**, *68*, 1500.
(24) Yelin, D.; Meshulach, D.; Silberberg, Y. *Opt. Lett.* **1997**, *22*, 1793.
(25) Baumert, T.; Brixner, T.; Seyfried, V.; Strehle, M.; Gerber, G. *Appl. Phys. B* **1997**, *65*, 779.
(26) Efimov, A.; Moores, M. D.; Beach, N. M.; Krause, J. L.; Reitze, D. H. *Opt. Lett.* **1998**, *23*, 1915.
(27) Brixner, T.; Strehle, M.; Gerber, G. *Appl. Phys. B* **1999**, *68*, 281.
(28) Bardeen, C. J.; Yakovlev, V. V.; Wilson, K. R.; Carpenter, S. D.; Weber, P. M.; Warren, W. S. *Chem. Phys. Lett.* **1997**, *280*, 151.
(29) Assion, A.; Baumert, T.; Bergt, M.; Brixner, T.; Kiefer, B.; Seyfried, V.; Strehle, M.; Gerber, G. In *Ultrafast Phenomena XI*; Elsaesser, T., Fujimoto, J. G., Wiersma, D. A., Zinth W., Eds.; Springer Series in Chemical Physics; Springer: Berlin, 1998; Vol. 63, p 471.
(30) Assion, A.; Baumert, T.; Bergt, M.; Brixner, T.; Kiefer, B.; Seyfried, V.; Strehle, M.; Gerber, G. *Science* **1998**, *282*, 919.
(31) Meshulach, D.; Silberberg, Y. *Nature* **1998**, *396*, 239.
(32) Weiner, A. M.; Leaird, D. E.; Patel, J. S.; Wullert, J. R. *Opt. Lett.* **1990**, *15*, 326.
(33) Weiner, A. M.; Leaird, D. E.; Patel, J. S.; Wullert, J. R. *IEEE J. Quantum Electron.* **1992**, *28*, 908.
(34) Wefers, M. M.; Nelson, K. A. *J. Opt. Soc. Am. B* **1995**, *12*, 1343.
(35) Dugan, M. A.; Tull, J. X.; Warren, W. S. *J. Opt. Soc. Am. B* **1997**, *14*, 2348.
(36) Mamyrin, B. A. *Int. J. Mass Spectrom. Ion Processes* **1994**, *131*, 1.
(37) Bañares, L.; Baumert, T.; Bergt, M.; Kiefer, B.; Gerber, G. *J. Chem. Phys.* **1998**, *108*, 5799.
(38) Letokhov, V. S. *Phys. Today* **1977**, *30*, 23.
(39) Zewail, A. H. *Phys. Today* **1980**, *33*, 27.
(40) Jortner, J., Levine, R. D., Rice, S. A., Eds. *Photoselective Chemistry*; Adv. Chem. Phys.; Wiley: New York, 1981; Vol. 47.
(41) Bloembergen, N.; Zewail, A. H. *J. Phys. Chem.* **1984**, *88*, 5459.
(42) Bañares, L.; Baumert, T.; Bergt, M.; Kiefer, B.; Gerber, G. *Chem. Phys. Lett.* **1997**, *267*, 141.
(43) Goldberg, D. E. *Genetic Algorithms in Search, Optimization, and Machine Learning*; Addison-Wesley: Reading, MA, 1993.
(44) Schwefel, H.-P. *Evolution and Optimum Seeking*; Wiley: New York, 1995.
(45) Rubner, O.; Baumert, T.; Bergt, M.; Kiefer, B.; Gerber, G.; Engel, V. *Chem. Phys. Lett.*, submitted for publication.